Role of agitation in the freezing process of liquid foods using sucrose aqueous solution as a model liquid

Role of agitation in the freezing process of liquid foods using sucrose aqueous solution as a model liquid

Hayato Masuda, Tomohiro Ryuzaki, Hiroyuki Iyota

Citation	Journal of Food Engineering. 330; 111100
Issue Date	2022-10
Version of Record	2022-04-25
Type	Journal Article
Textversion	Author
Rights	© 2022 Elsevier Ltd. This manuscript version is made available under the CC-BY-NC-ND 4.0 License. https://creativecommons.org/licenses/by-nc-nd/4.0/. This is the accepted manuscript version. The formal published version is available at https://doi.org/10.1016/j.jfoodeng.2022.111100.
DOI	10.1016/j.jfoodeng.2022.111100

Masuda, H., Ryuzaki, T., and Iyota, H. (2022). Role of agitation in the freezing process of liquid foods using sucrose aqueous solution as a model liquid. *Journal of Food Engineering*, 330, 111100. https://doi.org/10.1016/j.jfoodeng.2022.111100

Title:

Role of agitation in the freezing process of liquid foods using sucrose aqueous solution as a model liquid

Authors:

Hayato Masuda*, Tomohiro Ryuzaki, Hiroyuki Iyota

Affiliation:

Department of Mechanical and Physical Engineering, Osaka City University, 3-3-138 Sugimoto, Sumiyoshi-ku, Osaka 558-8585, Japan

Corresponding author:

* To whom corresponded should be addressed:

E-mail address: hayato-masuda@osaka-cu.ac.jp

Highlights

- The role of agitation in the freezing process was investigated.
- Samples frozen at a higher agitation speed tends to melt at a lower temperature.

- The degree of supercooling depends on the flow conditions.
- The time scale for the nucleation and growth of ice crystals was controlled by the agitation speed.

Keywords: Freezing process; Agitation; Supercooling degree; Ice crystal; Torque; Rheology

Abstract

Agitation is often encountered in various processes, such as ice cream manufacture and suspension freeze-concentration of liquid food. This study investigated the effect of agitation speed on the freezing process of an aqueous sucrose solution as a preliminary investigation for the development of processes that include both agitation and freezing. A batch-type freezer with an anchor impeller was used. Frozen samples at a higher agitation speed started to melt at a lower temperature. In addition, the degree of supercooling tended to increase along with the Reynolds number. In other words, it is possible to control the supercooling phenomenon, which is regarded as a stochastic phenomenon, based on the agitation operation. Furthermore, the time scale for the nucleation and growth of ice crystals depended on the agitation speed. Thus, it was concluded that the agitation operation significantly affects freezing process of sucrose aqueous solution with the batch-type freezer.

1. Introduction

In many food processing operations, the flow field, including temperature and concentration distributions, in the apparatus is quite complicated, because the physicochemical state of food changes during processing. Rheological properties typically change, which is accompanied by thermomechanical protein denaturation (Shimoyamada et al., 2019) and formation of network structure such as starch gelatinization (Matsumoto et al., 2021). These changes in rheological properties considerably affect the fields (flow, temperature, and concentration). From the viewpoint of food engineering, one of the most critical field changes is phase change; for example, boiling, condensation, evaporation, solidification, and melting. Boiling and condensation are popular heating processing and cooking processes. Therefore, a lot of studies have focused on heat transfer characteristics during heating and final food quality, e.g. Alhama and González Fernández (2002), Luo et al. (2015), and Zou et al. (2021). Similarly, cooling operations for freezing food have been investigated by many researchers. One of the most attractive areas in cooling processing is the manufacture of frozen food. The effect of freezing conditions on the quality of various foods has been reported by many researchers, including Olivera and Salvadori (2009), Chassagne-Berces et al. (2010), Cartagena et al. (2021), and Yang et al. (2021). In addition, it is known that novel energetic methods, such as ultrasound or pulse magnetic field, have been applied to the freezing process to improve efficiency (Tian et al., 2020; Zhang et al., 2021). In addition, new techniques have been developed to assess freezing processes. Kono et al. (2021) proposed a contactless method for monitoring the food freezing process using microwave resonance spectroscopy. Goñi et al. (2008) applied a genetic algorithm approach to predict food freezing and thawing times.

However, these researches were limited to static freezing, that is, without convection. Dynamic freezing with forced convection is also important in food processing. For example, in ice cream manufacturing process, an ice cream mix is aggressively agitated in a freezer. Masuda et al. (2020) and Sawano et al. (2021) reported that the agitation speed in a batch-type freezer significantly affects the internal structure of ice cream, including bubble/fat globule size distribution. Agitation during freezing is also used in suspension freeze-concentration, which is known as an efficient separation method from a viewpoint of heat transfer. Qin et al. (2007) and Ding et al. (2021) reported that agitation by a rotor with scraper is a dominant factor for heat transfer and the ice production rate during suspension freeze-concentration. Thus, although the effect of forced convection on the freezing process should be investigated, little research has been conducted on this topic. Arora and Howell (1973) investigated the freezing phenomenon of water in a pipe flow and reported that the degree of supercooling, which significantly affects the ice crystal size, clearly depends on the flow condition in the tube. Brooks et al. (2020) found that the flow condition in a helical coiled heat exchanger is one of important parameters for freezing process of sodium chloride aqueous solutions. A similar tendency is expected for freezing using a stirred vessel. For example, Shirai et al. (1985) proposed a kinetic model for ice crystallization to predict ice crystal growth. However, the effect of agitation on the freezing process is not comprehensively understood because they kept the agitation speed constant at 600 rpm. Therefore, the investigation of the effect of agitation on freezing processing is valuable for food engineers.

The objective of this study is to preliminarily investigate the effect of agitation speed on the freezing process from a practical viewpoint, particularly supercooling phenomenon and ice crystal growth process. A commercial batch-type freezer was used in this study. A sucrose aqueous solution was selected as the model liquid. The temperature and torque changes with time were measured during freezing. Findings and results obtained in this study will be utilized to optimize the agitation operation mainly in the manufacturing process of ice cream or the suspension freeze-concentration process.

2. Materials and methods

2.1 Experimental apparatus

A batch-type freezer (ICE-100, Cuisinart) with a vessel with 0.144 m diameter and 0.107 m height was used, as shown in Fig.1. A shaft, a torque meter (TPS-A-05NM, Kyowa Electric Co., Ltd.), and an anchor-type impeller [diameter (D): 0.140 m, height (H): 80 mm, thickness: (d) 10 mm] was attached to a stirrer (EUROSTAR 200 control, IKA). A K-type sheathed thermocouple with a diameter of 1 mm was attached to the surface 20 mm from the bottom surface. Thus, the liquid temperature near the cooling surface was measured. Because the surface state, including roughness significantly affected the supercooling phenomenon, the vessel was washed thoroughly after every experiment. A 400-mL sucrose aqueous solution (concentration C = 10, 25, 50 wt%) of 4 °C was added, and the liquid was cooled and agitated simultaneously. The agitation speed (N) was varied from 10 to 90 rpm. The liquid height was set at 30 mm. The liquid temperature and torque were recorded using a data logger (mini LOGGER GL200, GRAPHTEC). The flow was recorded using a video camera during the freezing process. Agitation was conducted until the torque reached the rated torque (0.50 N·m). Each experiment was performed three or four times, and the average values are shown in each figure.

2.2 Measurement of rheological properties

After freezing, the rheological properties of the frozen samples were measured using a stress-controlled rheometer (MCR102, Anton Paar GmbH) with a parallel plate with a diameter of 25 mm. The sample was taken from the freezer 30 minutes after the start of cooling/agitation and immediately placed on the sample stage of the rheometer, whose surface temperature was maintained at –10°C. To prevent heat transfer with the environment, the plate and stage were spatially covered by the hood, into which a Peltier element was mounted.

During the measurement, the temperature of the sample stage was increased from –10°C to 5°C at a heating rate of 0.5 °C/min. Simultaneously, the oscillation test was performed at a constant amplitude deformation, γ, 1×10^{4}, and angular frequency, ω, 10 1/s. It was confirmed beforehand that this measurement condition was within the linear viscoelastic regime of the sample.

2. 3 Conversion from temporal change in torque to that in viscosity during freezing

The temporal change in viscosity during freezing, which is an important factor for design of agitation device, is basically related to the temporal change in agitation torque. To investigate the power characteristics of the batch-freezer with the impeller, the power number-Reynolds number correlation was experimentally constructed, as shown in Fig. 2. The power number, N_p, and Reynolds number, Re, were calculated as follows:

$$N_p = \frac{P}{\rho N^3 D^5} \tag{1}$$

$$Re = \frac{D^2 \left(\frac{N}{60}\right) \rho}{\mu} \tag{2}$$

, where P is the power consumption [W], ρ [kg/m^3] is the fluid density, and μ [Pa·s] is the fluid viscosity.

Aqueous glycerol solutions of various concentrations were used to construct the N_p-Re correlation. The measurement of N_p under a wide Re range condition was realized using glycerol solutions of various concentrations because the viscosity of glycerol solutions widely varies with its concentration. It should be noted that the N_p-Re correlation curve is inherent to the stirred vessel. This means that the correlation does not depend on fluid viscosity and density. The N_p-Re correlation curve is useful for the conversion of the change in torque with time to the change in viscosity. The procedure was as follows: (i) the change in the torque with time during freezing was continuously measured; (ii) the torque changes were converted to the N_p change based on Eq. (1); (iii) the Re corresponding to the value of N_p was estimated from Fig. 2; (iv) the viscosity was calculated from Eq. (2). This method was proposed by Metzner and Otto (1957), and its concept has been approved by many researchers, such as Anne-Archard et al. (2006) and

Kaminoyama et al. (2011). The Metzner-Otto concept is mainly utilized for not only liquid mixing but also slurry agitation (Herman et al., 2012; Edifor et al., 2021). The definition of viscosity of frozen material is quite complicated. Nevertheless, the apparent viscosity estimated by the Metzner-Otto concept can be regarded as the “average” viscosity which is practically essential to the development of agitation equipment such as the agitation blade and the motor.

It is well known that N_p is inversely proportional to Re in the laminar flow region and approaches a constant value in the turbulent flow region. As shown in Fig. 2, the flow condition in the freezer is determined as follows: laminar flow when $Re \leq 100$, transition flow when $100 < Re \leq 7000$, and turbulent flow when $Re > 7000$. The N_p-Re correlation equations at each flow region are as follows:

$$\text{(Laminar flow region, } Re \leq 100) \qquad N_\mathrm{p} = \frac{160}{Re} \tag{3}$$

$$\text{(Transition flow region, } 100 < Re \leq 7000) \qquad N_\mathrm{p} = \frac{33}{Re^{0.61}} \tag{4}$$

$$\text{(Turbulent flow region, } Re > 7000) \qquad N_\mathrm{p} = \frac{3.3}{Re^{0.33}} \tag{5}$$

It was confirmed that, in all flow regions, N_p can be adequately estimated within a ±15% error using Eqs. (3)–(5).

2. 4 Statistical analysis

Statistical analysis was conducted if the tendency should be compared between each experimental condition. Experimental data were subjected to a one-way ANOVA test. The significance level of $p \leq 0.05$ was selected for all tests.

3. Results and discussion

Figure 3 shows the change in temperature and torque with time at C = 25 wt% and N = 30 rpm. In all conditions (N and C), the aqueous sucrose solution was frozen in the supercooled state. The degree of supercooling, ΔT_d, is defined as the difference between the minimum temperature in the supercooling state and the freezing temperature. It was confirmed that the torque increased suddenly after the supercooling state was released. Based on temperature, torque, and appearance, the freezing process can be classified into three states: liquid, slurry, and mushy, as shown in Fig. 4. The final state of the frozen solution was more solid than the liquid. Quantitatively understanding the changes in the rheological properties of solutions during freezing is valuable for food engineers. The apparent viscosity can be estimated from the power consumption associated with agitation.

As a typical example, Figure 5 shows the change in viscosity with time during freezing at C = 25 wt% and N = 10, 30 and 90 rpm. In all cases, the viscosity rapidly increased after the release of supercooling. In addition, the behavior of the increase in viscosity with time depended on the agitation speed. Especially, the increase at N = 90 rpm was more gentle than other two cases (N = 10 and 30 rpm). Higher agitation suppresses that ice crystals locally grow due to the enhanced dispersion of ice nuclei generated. This leads to the gentle increase in viscosity. On the other hand, in the case of relatively low agitation (N = 10 and 30 rpm), frozen materials accumulate at the front of agitation without breakdown or dispersion because of poor dispersion, as shown in Fig. 4 (c). Understanding the viscosity increase at various conditions (C and N) is essential for developing a freezer with an agitation impeller.

In addition, the effect of agitation speed on the rheological properties of frozen products is also an important factor from a practical viewpoint. In the case of C = 25 wt%, Figure 6 presents the storage modulus obtained by thermo-oscillatory measurement with sample heating 30 min after the start of cooling/agitation at N = 30 and 60 rpm. In each sample, there was no clear difference in the value of storage modulus in the solid and liquid states. Nevertheless, the melting temperature, at which the storage modulus at N = 60 rpm started to decrease, seemed to be lower than that at N = 30 rpm. Higher agitation speed induced ice crystal micronization. As a result, it is inferred that a micronized ice crystal with a larger specific interfacial area has a lower thermal resistance. Although the ice crystal size should be measured in the future, Sawano et al. (2021) reported a similar tendency, as the ice cream prepared at a higher agitation speed in a batch freezer showed a larger melting rate. Because only two conditions are compared in Fig. 6, further investigation at various parameters (*N* and *C*) is necessary to conclude the tendency. Nevertheless, it is inferred that the agitation speed is an important factor in controlling the rheological and thermal properties of frozen products.

The effect of flow condition on the freezing process was investigated, and Figure 7 shows the effect of *Re* on the supercooling degree (ΔT_d). The physical properties of the solution measured at 4°C were used to calculate *Re*. The results are tabulated in Table 1, and one-way ANOVA was implemented. It is noted that the representative *Re* should be considered because *Re* temporally changes with the viscosity during freezing. However, the measurement of physical properties below the freezing temperature are technically difficult due to partial/complete freezing. Thus, the values at 4°C was selected as the representative values. It is noted that significant local supercooling at the cooling surface was not observed in the recorded image and movie due to the periodic scraping by the impeller.

In the case of C = 10 wt%, ΔT_d seems to be independent of *Re*. On the contrary, when

$700 < Re < 10000$, ΔT_d monotonically increased with *R*e in the case of $C = 25$ and 50 wt%. Although the reason for this different tendency remains unclear, this could be explained by the difference in the intermolecular interaction according to the sucrose concentration because the supercooling phenomenon is basically dominated by the interaction between molecules (Kang et al., 2020). With respect to the case of $C = 25$ and 50 wt%, transition or turbulent flow conditions promote supercooling. This result is in agreement with the forced-convection system results using water in a pipe (Arora and Howell, 1973). Although the simple comparison with their study is not suitable because of the difference in the experimental system and working fluids, fluid flow is considered to be one of the factors that contribute to the supercooling phenomenon when the solution is not dilute, e.g. $C \geq 25$ wt%. One of the possibilities for supercooling promotion at higher *Re* is that the temperature distribution in the vessel becomes uniform at a higher *Re*. Although the temperature distribution at a relatively higher *Re* is not considered very remarkable, the small nonuniformity would affect microscale phenomena, such as supercooling. Another possibility is that the unsteady disturbance in the velocity component of the transition/turbulent flow has a positive effect for keeping the supercooling state. To keep the supercooled liquid state, water molecules should behave as liquid without phase change to solid. Higher kinetic energy input to the solution under higher *Re* may help molecules actively motion keeping liquid state even under the thermodynamically unstable condition. This microscopic assumption would be revealed by molecular dynamics (MD) simulations. Kawasaki and Kim (2017) pointed out that the viscosity relates to the supercooling phenomenon using MD simulations. Actually, the viscosity of sucrose aqueous solution at 4°C is 0.0019 Pa·s (C = 10 wt%), 0.0038 Pa·s (C = 25 wt%), and 0.0286 Pa·s (C = 50 wt%). In the future, MD simulations would also help to clarify the effect of sucrose concentration on the supercooling phenomenon. Although the supercooling phenomenon is somewhat stochastic (Shirai at al., 1986), control of the supercooling degree, which is a driving force for ice crystal growth, is a challenging topic. For example, Matsumoto et al. (2018) attempted to actively control the degree of supercooling by adding surfactants. As discussed above, flow condition is one of the parameters that contribute to the supercooling phenomenon. Further investigation is necessary to clarify effect of flow conditions in the future.

Figure 8 shows a snapshot of the state immediately after the release of supercooling at C = 25 wt% and N = (a) 10, (b) 30, (c) 60, and (d) 90 rpm, i.e. *Re* = (a) 860, (b) 2579, (c) 5158, and (d) 7737. In addition, ΔT_d was (a) 1.7, (b) 4.0, (c) 5.6, and (d) 8.0°C. As clearly shown in Fig. 8, a higher ΔT_d leads to a larger amount of the frozen phase. It is assumed that the amount of frozen phase, that is, the product of the ice crystal, is related to the sudden increase in torque after the release of supercooling, G_{Max}, which is observed around 420 s in Fig. 3. To assess the kinetics of ice crystal growth, the time scale was estimated from the change in torque with time. Figure 9 (a) shows the change in temperature and torque with time near the release of supercooling in the case of C = 25 wt% and N = 30 rpm. In this case, the degree of supercooling was 5.1°C. The discrepancy of ΔT_d from Fig. 8 (c) at the same experimental condition (C = 25 wt% and N = 30 rpm) is simply explained by the reproducibility of supercooling phenomenon. The ice nuclei were first observed around the supercooling temperature at t_a, as shown by the circles in Fig. 9 (b). After that, when the torque reached G_{Max}, the ice crystals appeared to grow sufficiently at t_b (Fig. 9 (c)). Thus, the time between t_a and t_b is regarded as the time scale for ice crystal nucleation and growth, t_i. It is noted that the temporal decrease in torque after the peak is due to the dispersion of ice crystals caused by agitation.

Figure 10 shows the effect of agitation speed on the time scale (t_i) at various C values. The results are tabulated in Table 2, and one-way ANOVA was implemented. It was found that the higher the concentration, the longer the time scale for ice crystal nucleation and growth. In addition, in all cases of C, t_i monotonically decreased with an increase in agitation speed. To generalize the kinetics of ice crystal growth in Fig. 10, the results are converted to the non-dimensional form as the effect of non-dimensional time, t_i* [=

$t_i \cdot (N/60)$], on *Re*, as shown in Fig. 11. t_i* means the required number of impeller rotation for ice crystal nucleation and growth. Figure 11 shows that, in the case of C = 25 and 50 wt%, the non-dimensional time scale for ice crystal nucleation and growth increased with *Re* up to a certain *Re* which depends on the sucrose concentration (C), and then decreased. This result indicates that ice crystal nucleation and growth is significantly promoted above the certain *Re*. On the contrary, in the case of C = 10 wt%, the certain *Re* was not found within experimental conditions. Thus, it was found that the dynamics of ice crystal nucleation and growth depends on the sucrose concentration. Although a detailed model should be constructed by distinguishing primary/secondary nucleation in the future, the flow condition is considered one of the most important factors for ice crystal nucleation and growth in freezing process of sucrose aqueous solution.

4. Conclusions

This study investigated the effect of agitation on the freezing process of aqueous sucrose solutions at various concentrations using a batch-type freezer. From the thermo-oscillatory test, it was found that the frozen sample with higher agitation speed started to melt at a lower temperature. In addition, the agitation speed affected the degree of supercooling. The supercooling degree increased with the Reynolds number, *Re*, except in low concentrations of sucrose. There are two possibilities for this tendency: (i) the uniform temperature distribution and (ii) velocity fluctuation at higher *Re*.

Furthermore, the time scale for the nucleation and growth of ice crystals was estimated from the recorded movie and the change in torque with time. In all concentration systems, the time scale decreased with agitation speed. Except in low concentrations of sucrose, the non-dimensional time for ice crystal nucleation and growth increased with *Re* up to a certain *Re* which depends on the sucrose concentration, and then decreased. This result indicates that ice crystal nucleation and growth is significantly promoted above the certain *Re*. Thus, agitation speed is one of the dominant factors in the ice crystal growth process.

Acknowledgements

This research was partially supported by JSPS KAKENHI (grant numbers 20K21110 and JP21K14450), and the Tojuro Iijima Foundation for Food Science and Technology.

Declaration of interest

The authors declare that they no conflict of interest.

Nomenclature

C	concentration [wt%]
D	diameter of impeller [m]
d	thickness of impeller [m]
G_{Max}	maximum torque immediately after release of supercooling [N·m]
H	height of impeller [m]
N	agitation speed [rpm]
N_{p}	power number [-]
P	power consumption [W]
Re	Reynolds number [-]
t_{a}	time at which ice nuclei were first observed [s]
t_{b}	time at which maximum torque was recorded after release of supercooling [s]
t_{i}	time scale for ice crystal nucleation and growth ($t_{\mathrm{b}} - t_{\mathrm{a}}$) [s]

Greek letters

ΔT_{d}	degree of supercooling [°C]
γ	deformation amplitude [-]
μ	fluid viscosity [Pa·s]
ρ	fluid density [kg/m^3]

ω angular frequency [1/s]

References

Alhama, F., González Fermández, C. F., 2002. Transient thermal behaviour of phase-change processes in solid foods with variable thermal properties. J. Food Eng. 54, 331–336.

Anne-Archard, D., Marouche, M., Boisson, H. C., 2006. Hydrodynamics and Metzner–Otto correlation in stirred vessels for yield stress fluids. Chem Eng. J. 125, 15–24.

Arora, A. P. S., Howell, J. R., 1973. An investigation of the freezing of supercooled liquid in forced turbulent flow inside circular tubes. Int. J. Heat Mass Transf. 16, 2077–2085.

Brooks, S., Quarini, G., Tierney, M., Yun, X., Lucas, E., 2020. Conditions for continuous ice slurry generation in a nylon helical coiled heat exchanger. Therm. Sci. Eng. Prog. 15, 100427.

Cartagena, L., Puértolas, E., Martínez de Marañón, I., 2021. Impact of different air blast freezing conditions on the physicochemical quality of albacore (Thunnus alalunga) pretreated by high pressure processing. LWT. 145, 111538.

Chassagne-Berces, S., Fonseca, F., Citeau, M., Marin, M., 2010. Freezing protocol effect on quality properties of fruit tissue according to the fruit, the variety and the stage of maturity. LWT 43, 1441–1449.

Ding, Z., Qin, F. G. F., Peng, K., Yuan, J., Huang, S., Jiang, R., Shao, Y., 2021. Heat and mass transfer of scraped surface heat exchanger used for suspension freeze concentration. J. Food Eng. 288, 110141.

Edifor, S. Y., Nguyen, Q. D., van Eyk, P., Biller, P., Hall, T., Lewis, D. M., 2021. Viscosity variation of model compounds during hydrothermal liquefaction under subcritical conditions of water. Ind. Eng. Chem. Res. 60, 980–989.

Goñi, S. M., Oddone, S., Segura, J. A., Mascheroni, R. H., Salvadori, V. O., 2008. Prediction of foods freezing and thawing times: Artificial neural networks and genetic algorithm approach. J. Food Eng. 84, 164–178.

Herman, C., Leyssens, T., Debaste, F., Hault, B., 2012. Detection of the II–I Etiracetam solvent-mediated polymorphic transformation through the online monitoring of the suspension apparent viscosity. J. Cryst. Growth 342, 57–64.

Kaminoyama, M., Nishi, K., Misumi, R., Otani, F., 2011. A method for determining the representative apparent viscosity of highly viscous pseudoplastic liquids in a stirred vessel by numerical simulation. J. Chem. Eng. Japan 44, 868–875.

Kang, T., You, Y., Jun, S., 2020. Supercooling preservation technology in food and biological samples: a review focused on electric and magnetic field applications. Food Sci. Biotechnol. 29, 303–321.

Kawasaki, K., Kim, K., 2017. Identifying time scales for violation/preservation of Stokes-

Einstein relation in supercooled water. Sci. Adv. 3, e1700399.

Kono, S., Imamura, H., Nakagawa, K., 2021. Non-destructive monitoring of food freezing process by microwave resonance spectroscopy with an open-ended coaxial resonator. J. Food Eng. 292, 110293.

Luo, L.-J., Guo, X.-N., Zhu, K.-X., 2015. Effect of steaming on the quality characteristics of frozen cooked noodles. LWT 62, 1134–1140.

Masuda, H., Sawano, M., Ishihara, K., Shimoyamada, M., 2020. Effect of agitation speed on freezing process of ice cream using a batch freezer. J. Food Process Eng. 43, e13369.

Matsumoto, K., Ueda, J., Ehara, K., Sakamoto, J., Furudate, Y., 2018. Active control of supercooling degree using two surfactants of different molecular sizes. Int. J. Refrig. 85, 462–471.

Matsumoto, M., Masuda, H., Hubacz, R., Horie, T., Iyota, H., Shimoyamda, M., Ohmura, N., 2021. Enzymatic starch hydrolysis performance of Taylor-Couette flow reactor with ribbed inner cylinder. Chem. Eng. Sci. 231, 116270.

Metzner, A. B., Otto, R. E., 1957. Agitation of non-Newtonian fluids. AIChE J. 3, 3–10.

Olivera, D. F., Salvadori, V. O., 2009. Effect of freezing rate in textural and rheological characteristics of frozen cooked organic pasta. J. Food Eng. 90, 271–276.

Qin, F. G. F., Premathilaka, Chen, X. D., Free, K. W., 2007. The shat torque change in a laboratory scraped surface heat exchanger used for making ice slurries. Asia-Pac. J. Chem. Eng. 2, 618–630.

Sawano, M., Masuda, H., Iyota, H., Shimoayamada, M., 2021. Melting characteristics of ice cream prepared with various agitation speeds in batch freezer. Chem. Eng. Trans. 87, 337–342.

Shimoyamada, M., Ishiyama, A., Masuda, H., Egusa, S., Matsuno, M., 2019. Viscosity changes of soymilk due to vacuum evaporation with moderate heating. LWT 112, 108255.

Shirai, Y., Nakanishi, K., Matsuno, R., Kamikubo, T., 1985. On the kinetics of ice crystallization in batch crystallizers. AIChE J. 31, 676–682.

Shirai, Y., Sakai, K., Nakanishi, K., Matsuno, R., 1986. Analysis of ice crystallization in continuous crystallizers based on a particle size-dependent growth rate model. Chem. Eng. Sci. 41, 2241–2246.

Tian, Y., Zhang, P., Zhu, Z., Sun, D-. W., 2020. Development of a single/dual-frequency orthogonal ultrasound-assisted rapid freezing technique and its effects on quality attributes of frozen potatoes. J. Food Eng. 286, 110112.

Yang, J., Zhang, B., Zhang, Y., Rasheed, M., Gu, S., Buo, B., 2021. Effect of freezing rate and frozen storage on the rheological properties and protein structure of non-fermented doughs. J. Food Eng. 293, 110377.

Zhang, L., Yang, Z., Deng, Q., 2021. Effects of pulsed magnetic field on freezing kinetics and physical properties of water and cucumber tissue fluid. J. Food Eng. 288, 110149.

Zhu, Z., Sun, D.-W., Zhang, Z., Li, Y., Cheng, L., 2018. Effects of micro-nano bubbles on the nucleation and crystal growth of sucrose and maltodextrin solutions during ultrasound-assisted freezing process. LWT 92, 404–411.

Zou, J., Xu, M., Zou, Y., Yang, B., 2021. Chemical compositions and sensory characteristics of pork rib and Silkie chicken soups prepared by various cooking techniques. Food Chem. 345, 128755.

Hayato Masuda: Conceptualization, Methodolgy, Validation, Investigation, Data Curation, Writing –Original Draft, Writing – Reviewing&Editing, Visualization, Project administration, Funding acquisition,

Tomohiro Ryuzaki: Methodolgy, Validation, Investigation, Data Curation

Hiroyuki Iyota: Methodolgy, Formal analysis

Figure 1. Experimental apparatus: (a) overview and (b) anchor impeller.

Figure 2. N_p-Re correlation curve for the freezer with the impeller. The N_p is inversely proportional in laminar flow region. Correlation curves is classified into three types according to flow regions: $N_p = 160/Re$ (laminar flow region, $Re \leq 100$), $N_p = 33/Re^{0.61}$ (transition flow region, $100 < Re \leq 7000$), $N_p = 3.3/Re^{0.33}$ (turbulent flow region, $Re > 7000$).

Figure 3. The changes in temperature and torque with time during freezing at C = 25 wt% and N = 30 rpm.

Figure 4. Snapshots of the state at C = 25 wt% and N = 30 rpm: (a) liquid, (b) slurry, and (c) mushy.

Figure 5 The change in the viscosity with time estimated using Metzner-Otto concept at C = 25 wt%.

Figure 6. Storage modulus of frozen samples obtained via a thermo-oscillatory test ($\gamma = 1\times10^4$, and ω = 10 1/s, and $\Delta T/t$ = 0.5 °C/min).

Figure 7. Effect of supercooling degree (ΔT_d) on Reynolds number (Re).

Figure 8. Representative snapshots of the state immediately after the release of supercooling at C = 25 wt%: (a) N = 10 rpm, Re = 860, ΔT_d = 1.7°C, (b) N = 30 rpm, Re = 2579, ΔT_d = 4.0°C, (c) N = 30 rpm, Re = 5158, ΔT_d = 5.6°C, and (d) N = 90 rpm, Re = 7737, ΔT_d = 8.0°C.

Figure 9. The change through supercooling at C = 25 wt% and N = 30 rpm: (a) the temporal change in temperature and torque, (b) the snapshot immediately before supercooling at t_a, and (c) immediately after supercooling at t_b. The circle in (b) presents the ice nuclei. In this experiment, the degree of supercooling was 5.1°C.

Figure 10. Effect of rotational speed of the impeller (N) on the time scale for ice crystal nucleation and growth (t_i).

Figure 11. Effect of Reynolds number (Re) on the non-dimensional time scale for ice crystal nucleation and growth (t_i*).

Figure 1

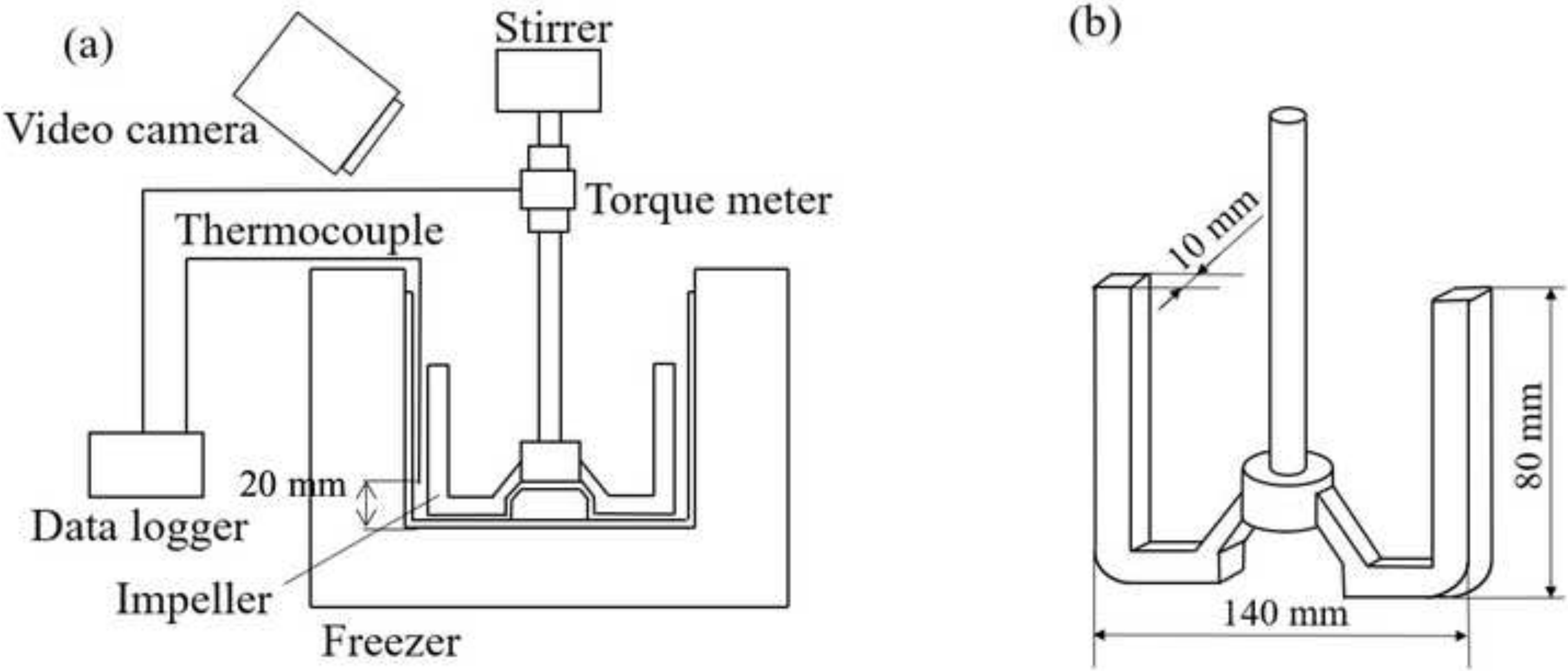

(a)
Video camera
Stirrer
Torque meter
Thermocouple
20 mm
Data logger
Impeller
Freezer
(b)
10 mm
80 mm
140 mm

Figure 2

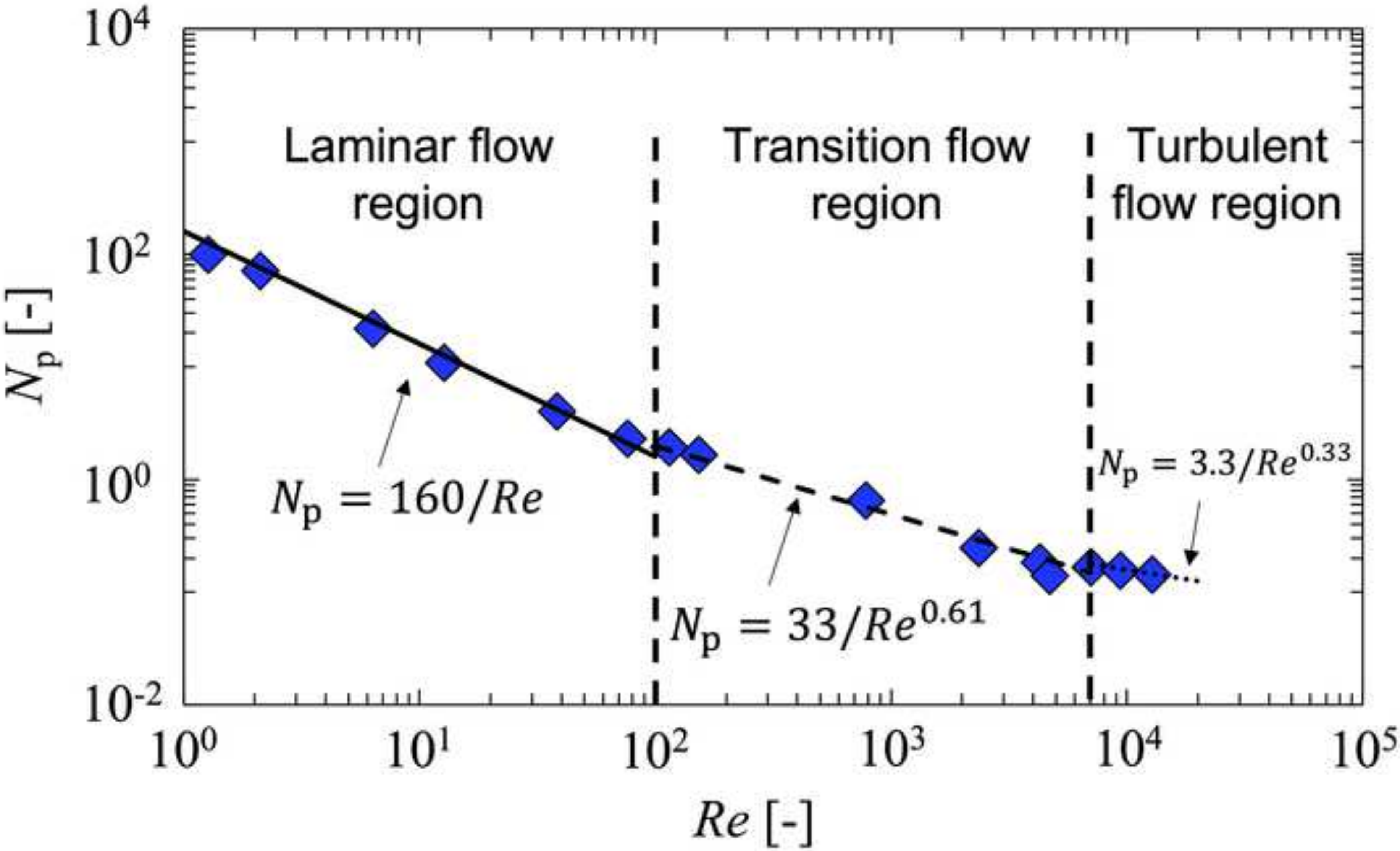

10^4
10^2
10^0
10^{-2}
N_p [-]
Laminar flow region
Transition flow region
Turbulent flow region
$N_p = 160/Re$
$N_p = 33/Re^{0.61}$
$N_p = 3.3/Re^{0.33}$
10^0
10^1
10^2
10^3
10^4
10^5
Re [-]

Figure 3

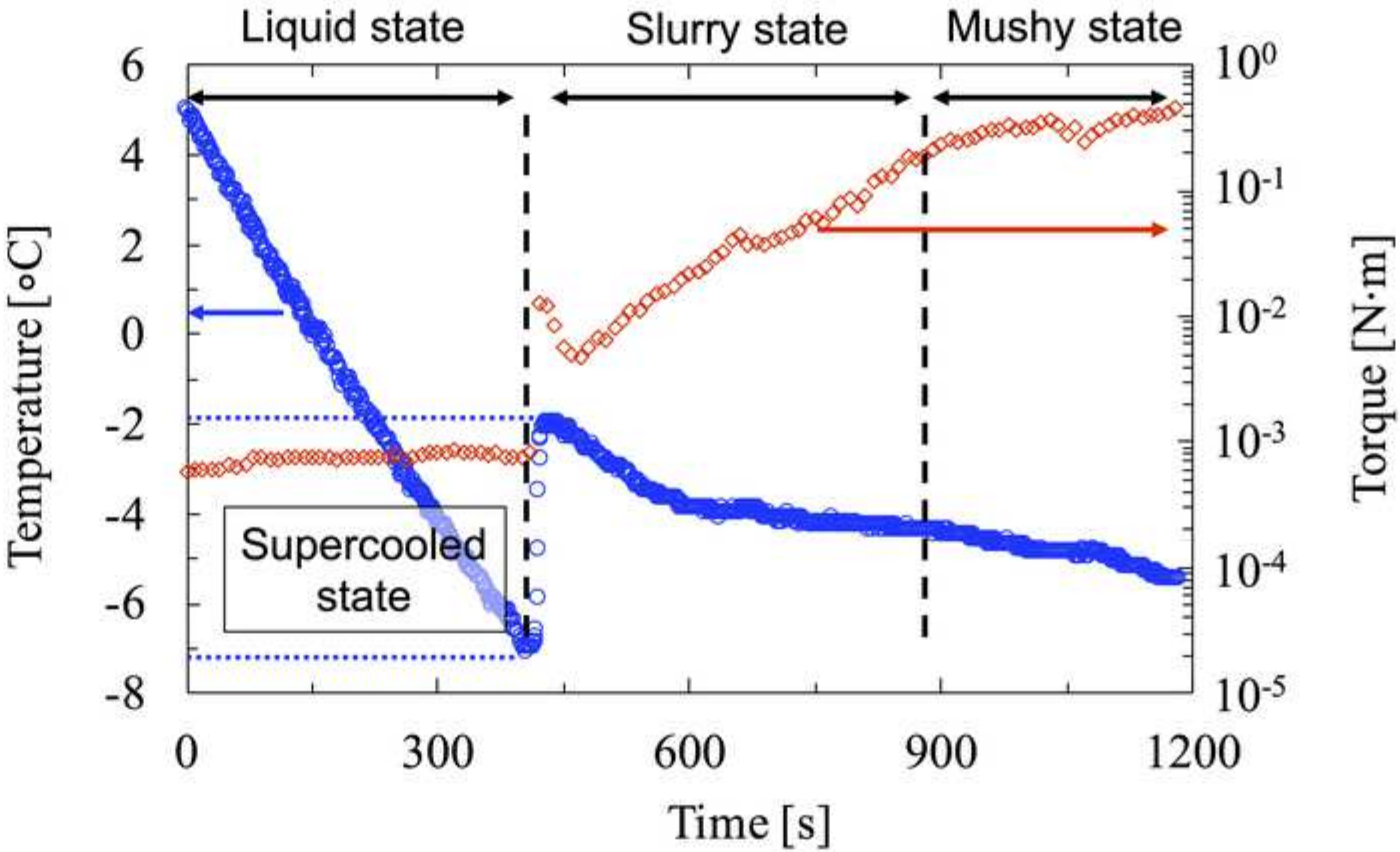

Liquid state
Slurry state
Mushy state
Supercooled state
Temperature [°C]
Torque [N·m]
Time [s]
6
4
2
0
-2
-4
-6
-8
0
300
600
900
1200
10^0
10^{-1}
10^{-2}
10^{-3}
10^{-4}
10^{-5}

Figure 4

Figure 5

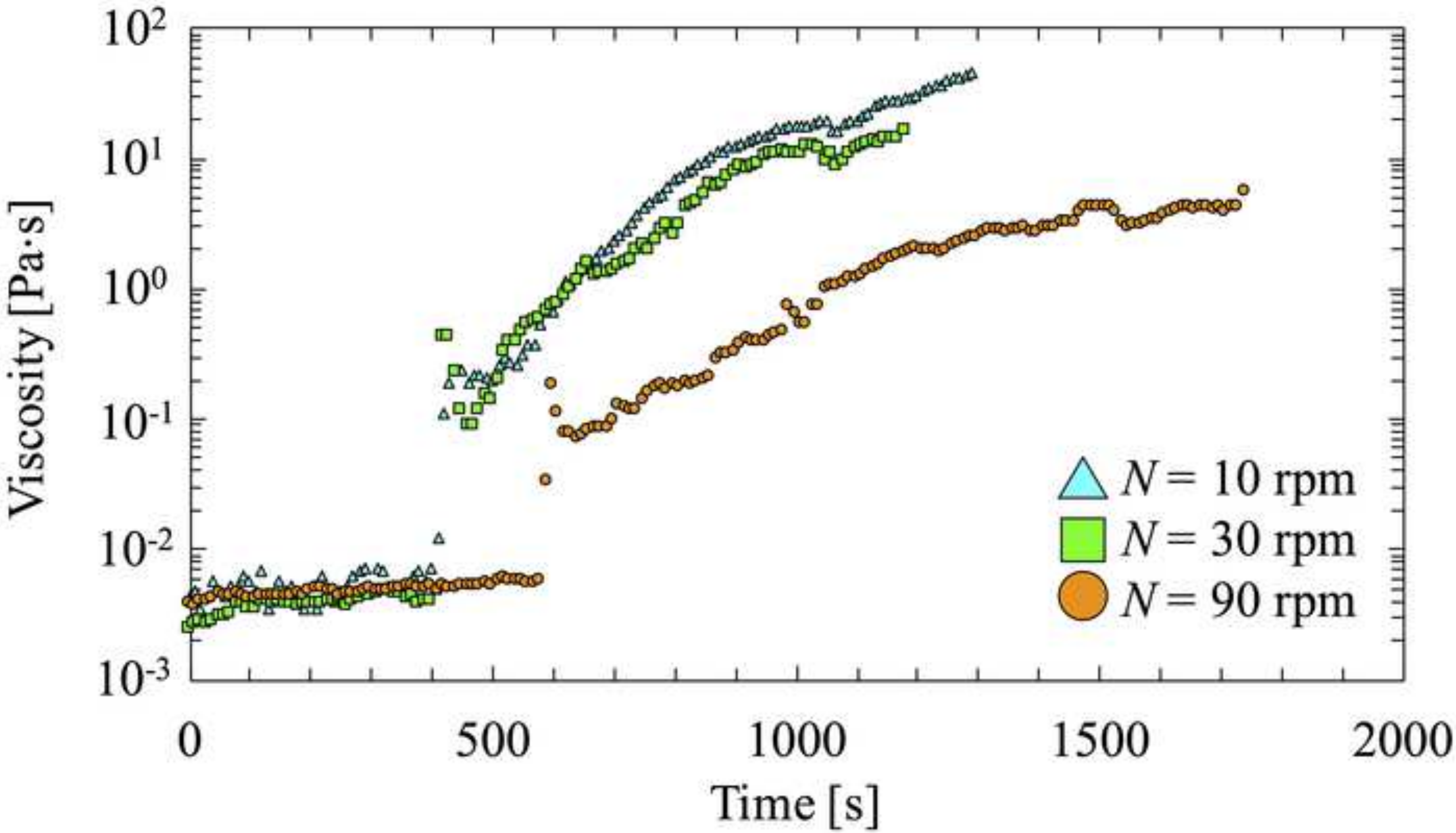

10^2
10^1
10^0
10^{-1}
10^{-2}
10^{-3}
Viscosity [Pa·s]
0
500
1000
1500
2000
Time [s]
N = 10 rpm
N = 30 rpm
N = 90 rpm

Figure 6

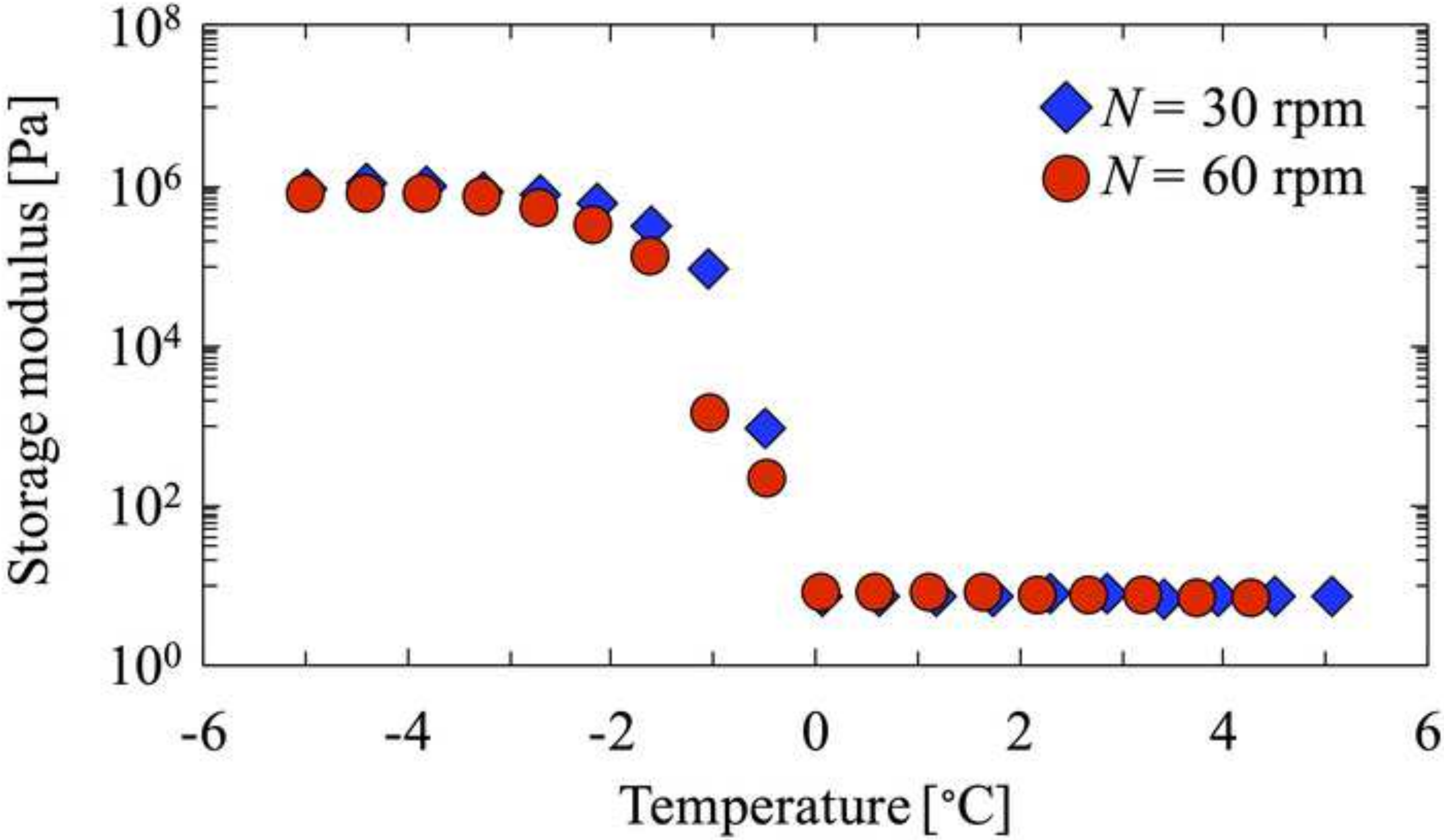

N = 30 rpm
N = 60 rpm
Storage modulus [Pa]
Temperature [°C]
10^8
10^6
10^4
10^2
10^0
-6
-4
-2
0
2
4
6

Figure 7

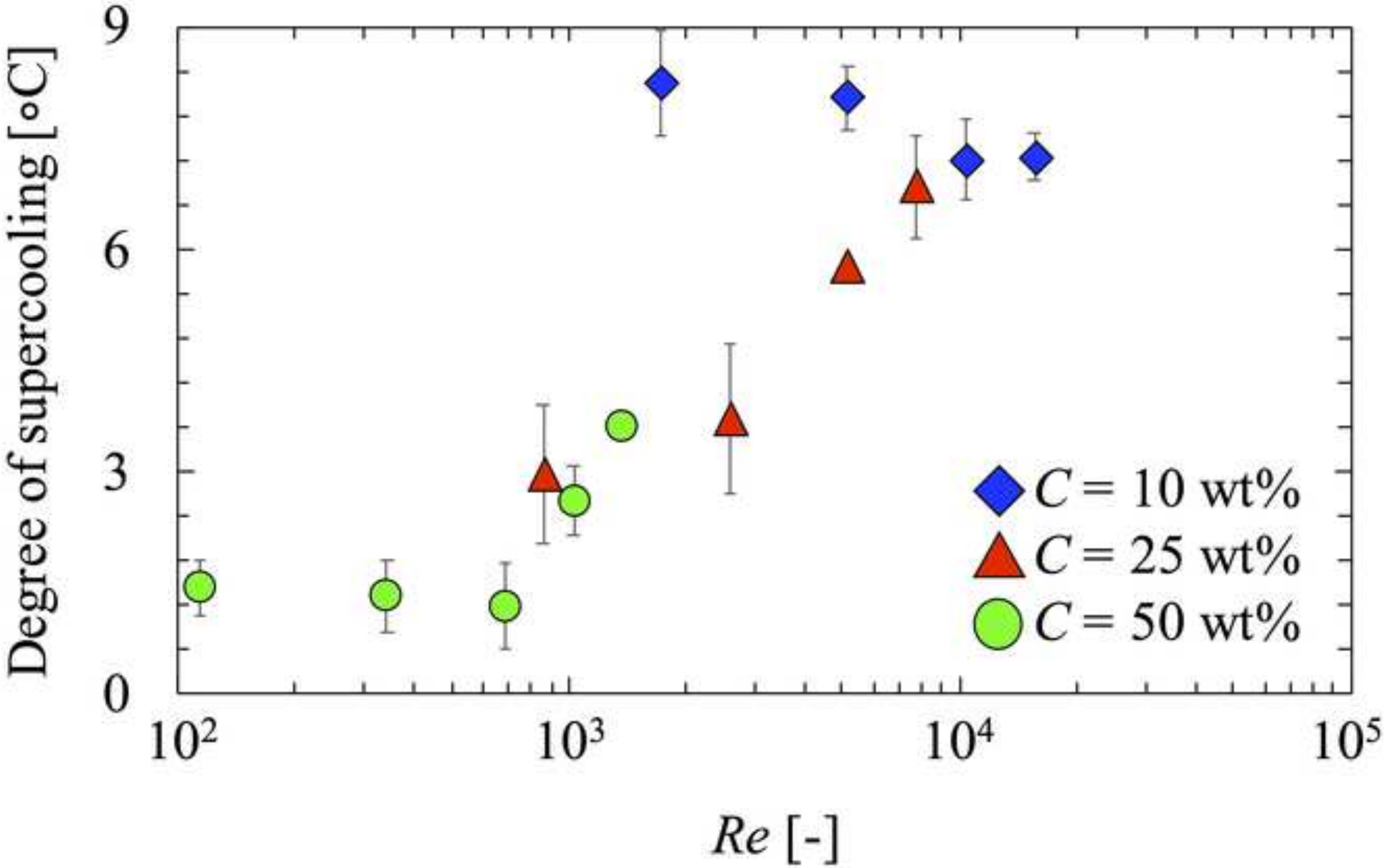

9
6
3
0
Degree of supercooling [°C]
10^2
10^3
10^4
10^5
Re [-]
C = 10 wt%
C = 25 wt%
C = 50 wt%

Figure 8

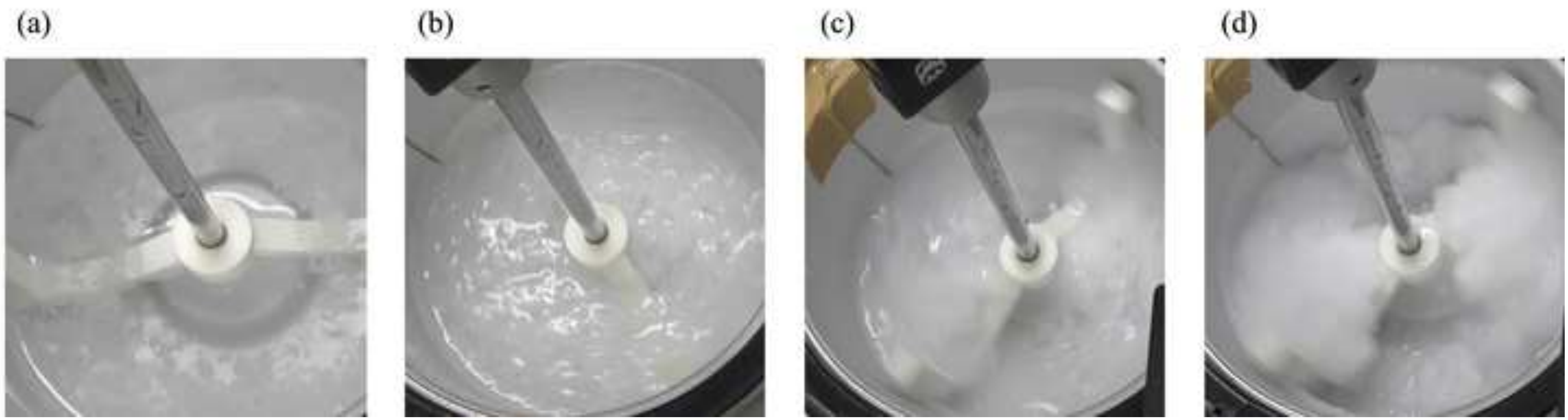

Figure 9

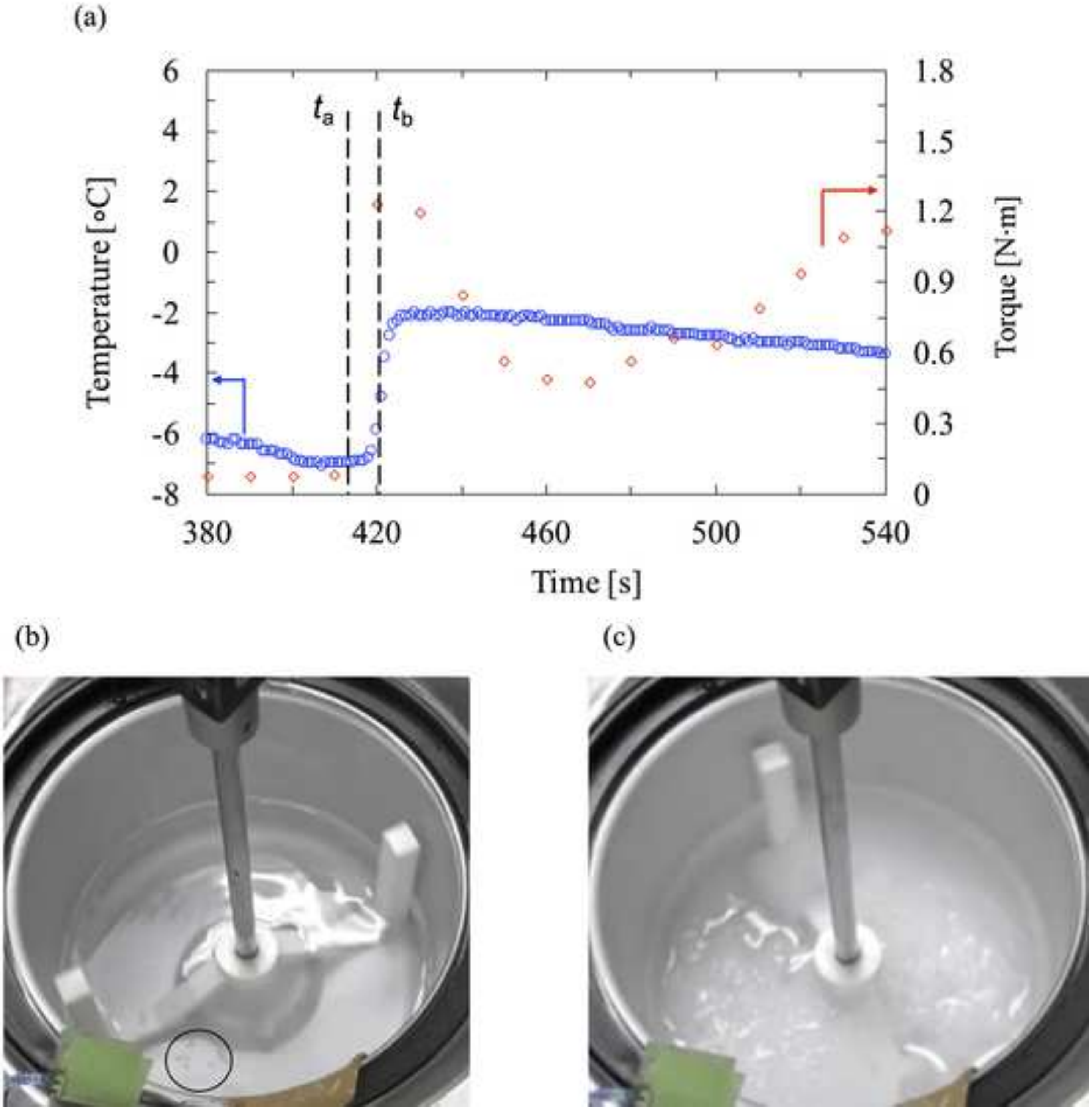

(a)
6
4
2
0
-2
-4
-6
-8
Temperature [°C]
1.8
1.5
1.2
0.9
0.6
0.3
0
Torque [N·m]
t_a
t_b
380
420
460
500
540
Time [s]
(b)
(c)

Figure 10

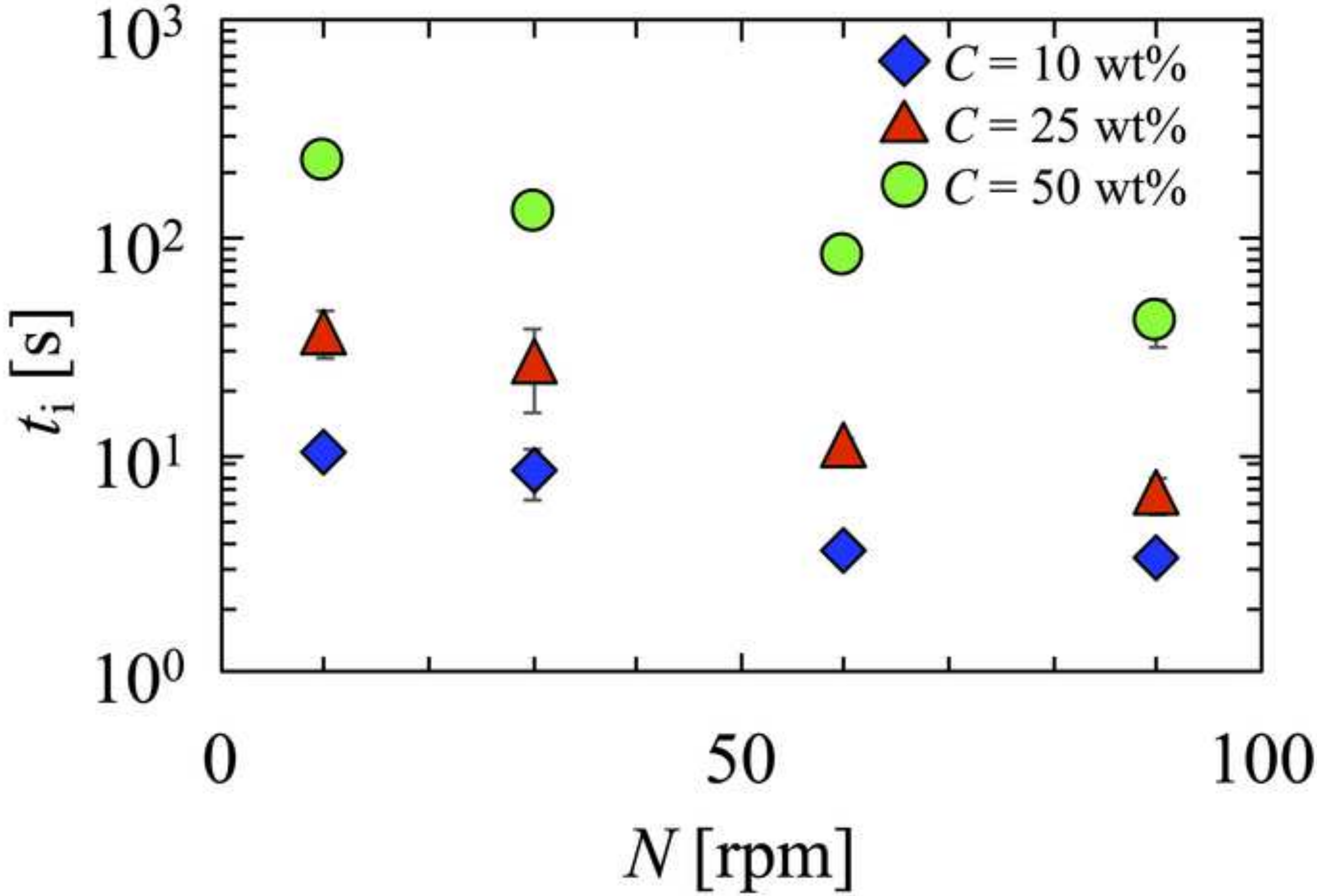

Figure 11

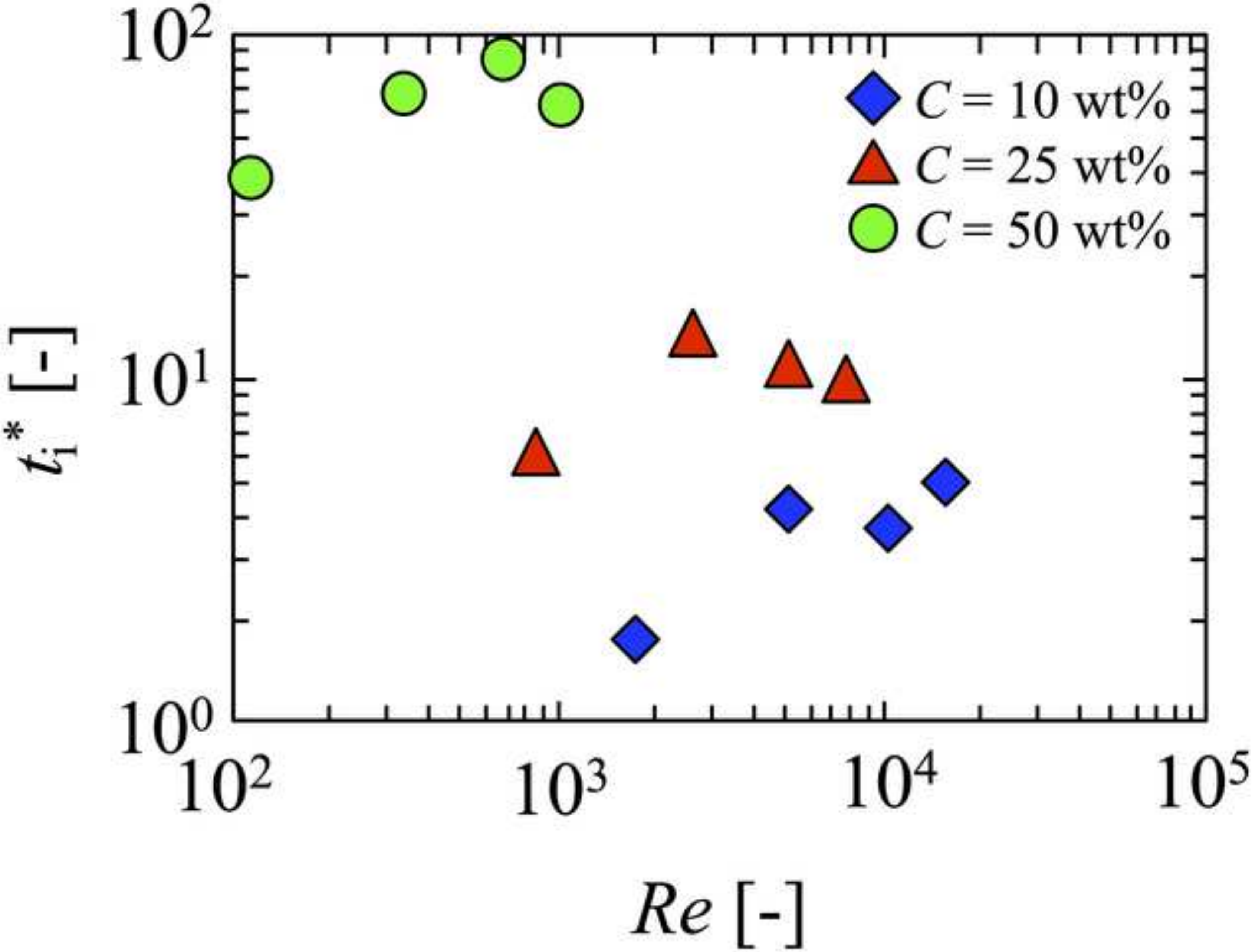

Table

Table 1 Degree of supercooling (ΔT_d) at different experimental conditions.

	C = 10 wt%		C = 25 wt%		C = 50 wt%	
N [rpm]	Re [-]	ΔT_d [°C]	Re [-]	ΔT_d [°C]	Re [-]	ΔT_d [°C]
10	1719	8.23 ± 0.70^{a}	860	2.97 ± 0.94^{b}	114	1.43 ± 0.37^{e}
30	5158	8.03 ± 0.44^{a}	2579	3.7 ± 1.02^{bc}	343	1.3 ± 0.49^{e}
60	10316	7.20 ± 0.53^{a}	5158	5.77 ± 0.08^{cd}	685	1.17 ± 0.58^{e}
90	15474	7.23 ± 0.33^{a}	7737	6.83 ± 0.69^{d}	1028	2.6 ± 0.47^{ef}
120	–	–	–	–	1370	3.6^{f}

Values are mean ± standard variation.

Values with the different superscript indicate significant difference ($p \leq 0.05$).

Table 2 Time scale for ice crystal nucleation and growth (t_i) at different experimental conditions.

	C = 10 wt%	C = 25 wt%	C = 50 wt%
N [rpm]	t_i [s]	t_i [s]	t_i [s]
10	10.33 ± 0.67^{a}	37.00 ± 9.02^{c}	227.33 ± 9.52^{e}
30	8.33 ± 2.19^{ab}	27.00 ± 11.37^{cd}	133.00 ± 7.00^{f}
60	3.67 ± 0.33^{b}	11.00 ± 1.00^{d}	83.33 ± 13.86^{g}
90	3.33 ± 0.33^{b}	6.67 ± 1.33^{d}	41.50 ± 9.50^{g}

Values are mean ± standard variation.

Values with the different superscript indicate significant difference ($p \leq 0.05$).